Motion Measurement Using Inertial Sensors, Ultrasonic Sensors, and Magnetometers With Extended Kalman Filter for Data Fusion

He Zhao and Zheyao Wang, *Member, IEEE*

***Abstract*—Inertial measurement units (IMUs) are widely used in motion measurement. However, the drift of IMUs results in significant accumulated errors for long-term position and orientation measurement. This paper reports a method to compensate the drift of inertial sensors with the assist of ultrasonic sensors and magnetometers. The magnetometer is combined with a three-axis accelerometer as a digital compass for orientation determination in static state by measuring the gravity and the earth's magnetic field vectors. A three-axis gyroscope is used to measure the orientation in dynamic state to complement the digital compass. Displacement determination is implemented using the accelerometer through double integration, and an ultrasonic sensor is employed to periodically calibrate the accumulated errors of the accelerometer. The redundant data from the multi-sensors are fused using extended Kalman filter (EKF), in which the position measured by the ultrasonic sensor and the orientation measured by the digital compass are defined as the observation values, and the position, velocity, and orientation are included in the state vector. Experimental results show that the accumulated errors of inertial sensors are reduced by ultrasonic sensors and magnetometers, and EKF improves the accuracy of orientation and position measurements.**

***Index Terms*—Data fusion, extended Kalman filter, inertial sensor, magnetometer, ultrasonic sensor.**

I. Introduction

With the advance in microfabrication technology, inertial measurement units (IMUs), which consist of a three-axis accelerometer and a three-axis gyroscope, have been widely used as the sensing unit for motion determination by measuring acceleration, velocity, displacement, angular rates, and rotation angles [1]. The prominent merits of IMUs, such as low cost, light weight, fast responsibility, and easy and self-contained operation, allow direct measurement of object motion without serious impact on system complexity, making them attractive to motion determination for small moving objects, such as mobile robots [2], handwriting pens [3], [4], hand-held tools [5], GPS [6], and vehicle navigation [6]–[8].

Manuscript received July 07, 2011; accepted August 17, 2011. Date of publication August 30, 2011; date of current version April 06, 2012. This work was supported by ABB Research and Tsinghua University Initiative Scientific Research Program 2009THZ01005. The associate editor coordinating the review of this manuscript and approving it for publication was Prof. Okyay Kaynak.

The authors are with the Institute of Microelectronics, Tsinghua University, Beijing 100084, China (e-mail: mhzapysy@yahoo.com.cn; z.wang@tsinghua.edu.cn).

Color versions of one or more of the figures in this paper are available online at http://ieeexplore.ieee.org.

Digital Object Identifier 10.1109/JSEN.2011.2166066

IMUs have good short-term precision and high sampling rates, but they suffer from serious errors in long-term position and orientation estimates due to the drift and the algorithm of integration [8]–[11]. The drift is inherent from the operation principles and the tiny effective vibrating mass of the inertial sensors, and is a major issue that limits the accuracy of inertial navigation. The primary parameters that IMUs measure are acceleration and angular rates, and other parameters including velocity, displacement, and rotation angles are obtained by integrating acceleration or angular rate over time. However, the drift and the integration errors lead to large accumulated errors in long-term motion determination, and even lead to divergent results. For long-term measurement, additional secondary position and orientation sensors are needed to complement IMUs to construct a hybrid system for drift compensation [10], [11]. Normal candidates for the secondary sensors include ultrasonic sensors [12], [13], laser range sensors [14], [15], cameras [16], GPS [17], and Doppler radars [18].

Ultrasonic sensors are one of the favorable complementary sensors for indoor localization due to the small size, light weight, and low cost. Ultrasonic sensors measure position through time-of-flight, triangulation, or phase coherence. Hybrid systems that use ultrasonic position sensors and IMUs have been developed to estimate position and orientation for industry control, robots, and consumer electronics [19]–[21]. For example, sonar sensors were used to track mobile robot pose to obtain occupancy grid maps [19]. A measurement system using a receiver mounted on the moving object and four ultrasonic emitters attached below a ceiling was developed for position determination [22]. The performance issues related to reflections, occlusions, and maximum emitting angles limit independent use of ultrasonic sensors.

Optical tracking systems, using cameras or laser assisted vision technology to record the trajectory of object, was developed for motion determination [9], [15], [23], [24]. When observing a known scene, both the position and the attitude of the camera can be obtained. By tracking visual features through sequences of images, the motion of the camera can be estimated. Hence cameras are able to localize position to compensate the drift errors of gyroscopes and accelerometers. Simultaneous localization and mapping were developed for inertial navigation by using vision-based technique to compensate inertial navigation divergence [25], in particular for vehicle navigation.

These multi-sensors give complementary and overlapping information as well as redundant, and data fusion, which is capable of optimizing the information from various redundant sen-

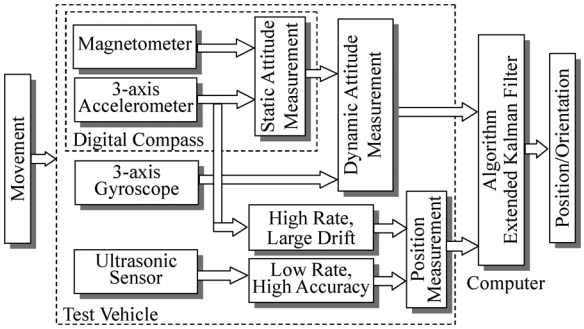

Fig. 1. Configuration of the sensor system.

sors, is employed to combine the information from multi-sensors of different types to reduce uncertainty. An approach for data fusion is Kalman filter (KF) [26], which can provide position and orientation in real-time. However it is applicable to linear systems, and suffers from linearization induced errors when applied to nonlinear systems. One method to solve the nonlinear problem is to use extended Kalman filter (EKF) [27]. For example, EKF has been used for orientation estimate for body segment [28] and road vehicle navigation with GPS and inertial navigation systems [29].

In this paper, we present a method to compensate the drift and the accumulated errors of inertial sensors using ultrasonic sensors and magnetometers for motion tracking. The contributions include two aspects. First, gyroscopes are used to extend the applicability of a digital compass in orientation determination from static state to dynamic state. Second, we use ultrasonic sensors in conjunction with accelerometers for position determination to compensate the drawbacks of each other, such as low sampling rate and large accumulated errors.

This paper is organized as follows. Section II describes the system configuration. Section III presents the ultrasonic sensor system for position calculation. In Section IV orientation determination using accelerometers and magnetometers is introduced. Section V gives the EKF algorithm and implementation for data fusion of the multi-sensors. Section VI reports the experimental results of motion tracking, as well as the comparison with a commercial product.

II. System Configuration

Fig. 1 shows the configuration and the operation principle of the proposed position and orientation measurement system. The system consists of a magnetometer, a three-axis accelerometer, a three-axis gyroscope, and an ultrasonic sensor. The magnetometer and the accelerometer constitute a digital compass, which is used to determine the inclination attitude in static state by measuring the gravity and the earth's magnetic field vectors [30]. The applicability of the digital compass is extended from static state orientation measurement to dynamic state by using gyroscopes. For position measurement ultrasonic sensors and accelerometers are combined to compensate the drawbacks of each other. All the sensor data are fused by EKF, which provides a critical function to balance and optimize the redundant information of the multiple sensors, such that the uncertainties in motion are minimized.

A. Principle of Orientation Measurement

In static state, roll and pitch angles can be obtained from the gravity components measured with the accelerometer. Due to the fact that the earth' magnetic field vector at arbitrary site is locally constant and always towards the magnetic north, magnetometers can be used to measure the components of the earth's magnetic field vectors to determine yaw (azimuth) [31], [32]. Therefore, the combination of an accelerometer and a magnetometer, so called a digital compass, can determine the orientation in static state through measuring the time-independent gravity and the earth's magnetic field vectors. Compared with gyroscopes, digital compasses do not suffer the drift and integration induced errors by providing an external reference to limit the bound drift [32]–[36], and are able to avoid drift errors, range limitations, and interference problems. The independency on artificially generated sources of digital compasses allows accurate orientation measurement, and it is emerging as an appealing technology for static state orientation determination [37]–[39].

Although digital compasses can determine orientation by measuring the gravity and the earth's magnetic field vectors, the fact that the accelerometers are sensitive to acceleration in any direction leads to orientation measurement errors when the object subjects to translational acceleration or fast rotation. If the amplitude of the translational acceleration is comparable to the gravity vector, or the object rotates at a relatively large angular rate, the preliminary condition of static state is invalid and the digital compass diverges rapidly. As gyroscopes are able to measure short-term angular rates at dynamic state, we propose to use gyroscopes to measure the transient orientation in dynamic state to compensate the digital compass, i.e., the digital compass measures the orientation in static state and the gyroscopes measure the short-term angular rates at dynamic state when subjected to fast rotation or translational acceleration.

B. Principle of Position Measurement

Conventionally displacement can be obtained through double integration of acceleration. However, the inevitable drift of accelerometers and the integration errors cause significant accumulated errors. To avoid this problem, we propose to use complementary ultrasonic sensors to provide redundant position information to calibrate the accelerometers.

The ultrasonic sensor consists of one emitter mounted on the moving object and three receivers fixed separately on the ground. By measuring the time delay between signal sending and receiving, distances between the emitter and the receiver and thus the absolute position of the object can be obtained. Although ultrasonic sensors have no accumulated errors and are quite accurate in position determination, the sampling rate of ultrasonic sensors is rather low due to the delay between sending and receiving. In addition, the movement of the emitter may render obstacles appearing on the path to the receivers, resulting in blind areas and thus occasional or frequent signal loss. Hence, ultrasonic sensors cannot be used independently for navigation applications from the reliability point of view.

Since the accelerometer has large drift but high sampling rate and the ultrasonic sensor has low drift but low sampling rate, in-

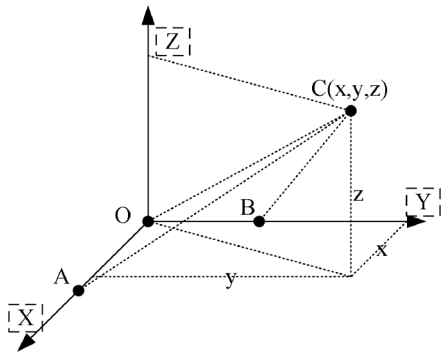

Fig. 2. Principle of ultrasonic sensors measurement system.

corporating the accelerometer and the ultrasonic sensor enables accurate position determination by compensating the disadvantages of each other. The ultrasonic sensor measures position periodically and the accelerometer operates during the intervals of two sequential ultrasonic signals to interpolate the relative positions. In such a manner, the ultrasonic sensor calibrates the accumulated errors of the accelerometer, and the accelerometer compensates the low sampling rate and signal loss of the ultrasonic sensor.

The gyroscope and the digital compass provide redundant orientation information, and the ultrasonic sensor and the accelerometer also offer redundant position information. The information from the multi-sensors overlaps or complements, and therefore an algorithm is needed to obtain the optimized information. This is accomplished by using extended Kalman filter (EKF) to fuse the measured data of the multi-sensors to obtain optimal results in terms of accumulated error, applicability, and frequency response.

III. Ultrasonic Sensor System

Fig. 2 shows the ultrasonic sensor system for position determination. It consists of one emitter mounted on the moving object, location $\mathrm{C}(x, y, z)$, and three receivers fixed separately at the origin O and two separate positions, A on the x-axis and B on the y-axis, with OA and OB known.

The distance s that the ultrasonic wave travels is given by

$$s = v(t_2 - t_1) \tag{1}$$

where $v = 331.5 + 0.6 \times \Delta T$ is the velocity of ultrasonic waves in the air, ΔT is the temperature difference between the operation and the reference temperature, t_1 and t_2 are, respectively, the time of signal sending and receiving. The strong temperature dependence and the relatively short traveling distance prevent the ultrasonic sensors from outdoor and long distance applications.

By measuring the time intervals between sending and receiving, the distances between the emitter and the three receivers can be obtained readily, and the absolute position of the point C at the fixed coordinate can be calculated using

$$\begin{cases} x^2 + y^2 + z^2 = OC^2 \\ x^2 + (OB - y)^2 + z^2 = BC^2 \\ (OA - x)^2 + y^2 + z^2 = AC^2 \end{cases} \tag{2}$$

After a time interval the object moves to a new position, of which the location can be obtained similarly. Therefore, the relative displacement of the object can be obtained by subtracting the current position from the initial position. The coordinate of the ultrasonic sensor should be in accordance with that of the attitude, as the position measured by the ultrasonic sensor is a part of data fusion algorithm.

As the ultrasonic wave could be reflected by other objects, the receivers may receive the reflected waves, resulting in interference in measurement. To avoid this problem, the time interval between two sequential ultrasonic signals is selected larger than the period for the ultrasonic wave to travel from the emitter to the receiver, such that the ultrasonic waves reflected once and more can be distinguished according to the receiving time and the magnitude of the received waves. This avoids the interference of reflected waves. Normally the ultrasonic waves travel a distance around 2–5 meters, so the time interval between sending and receiving is about 0.006–0.015 s. The program will make judgment when the ultrasonic receiver receives ultrasonic waves. This results in a low interrogating rate for ultrasonic sensors, and it is difficult to get sufficient positions to reconstruct a smooth motion trajectory when the object moves fast.

Accelerometers are employed to exploit the high dynamic response to measure the displacement by integrating the acceleration to interpolate two sequential positions measured by ultrasonic sensors. As the ultrasonic sensor is accumulated error free, it calibrates the drift and the accumulated errors of the accelerometer. In case of transient or short period of signal loss due to obstacles or emitting angle limit, the accelerometer replaces the ultrasonic sensor for independent position measurement before the ultrasonic signal is caught again. As the accumulated errors of the accelerometer increase with time, the largest acceptable error determines the longest tolerable period of signal loss. This complementary position measurement is implemented using EKF.

IV. Orientation Determination

In static state, roll and pitch can be calculated using coordinate transformation of the gravity vectors measured with accelerometers. As the geomagnetic vector is unaltered, the changes in the angle between the geomagnetic vector and the magnetic sensor represent the yaw angle. Therefore, an accelerometer and a magnetometer, i.e., a digital compass, are able to determine orientations by measuring the gravity and the geomagnetic vector. As the digital compass introduces no accumulated errors, it has been widely used for orientation determination in static state [40]–[43].

Fig. 3 shows the definition of the world frame and the body frame. The axes X_w, Y_w, and Z_w in the world frame correspond to the north, the east, and the upright directions, respectively, and X_b, Y_b and Z_b are the coordinates of the sensor body frame. Euler angles instead of quaternion [32] are employed for orientation determination for simplification. Rotation matrix method rather than Gauss-Newton [41] and QUEST [8] algorithms are

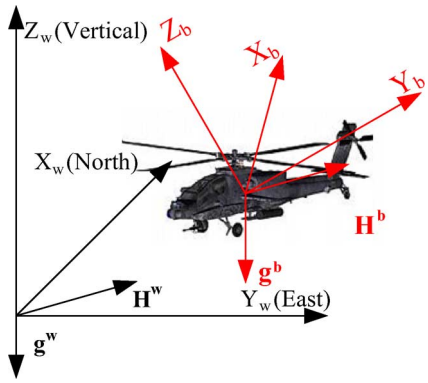

Fig. 3. World frame and body frame definition.

used to calculate the orientation using the gravity and the magnetic field vectors.

The gravity and the earth's magnetic field vectors in the world frame can be obtained using coordinate transformation from the body frame

$$g^w = R_b^w g^b \tag{3}$$
$$H^w = R_b^w H^b \tag{4}$$

where g and H represent the gravity and the earth's magnetic field vectors, respectively; the superscripts b and w denote the body frame and the world frame, respectively. R_b^w is the direction cosine matrix (DCM) from the body frame to the world frame, and can be expressed by the Euler angles, roll φ, pitch θ, and yaw ψ

$$R_w^b(\theta) = \begin{bmatrix} \mathrm{c}\theta\mathrm{c}\psi & \mathrm{c}\theta\mathrm{s}\psi & -\mathrm{s}\theta \\ \mathrm{s}\varphi\mathrm{s}\theta\mathrm{c}\psi - \mathrm{c}\varphi\mathrm{s}\psi & \mathrm{s}\varphi\mathrm{s}\theta\mathrm{s}\psi + \mathrm{c}\varphi\mathrm{c}\psi & \mathrm{s}\varphi\mathrm{c}\theta \\ \mathrm{c}\varphi\mathrm{s}\theta\mathrm{c}\psi + \mathrm{s}\varphi\mathrm{s}\psi & \mathrm{c}\varphi\mathrm{s}\theta\mathrm{s}\psi - \mathrm{s}\varphi\mathrm{c}\psi & \mathrm{c}\varphi\mathrm{c}\theta \end{bmatrix} \tag{5}$$

where c is defined as cos(), and s is defined as sin().

Since the world frame provides a reference frame to the object, the initial state of the object is defined when the body frame is completely consistent with the world frame. This means that the x-, y-, and z-axis point to the north, the east, and the upright, respectively. The initial gravity vector and the earth's magnetic field vector in the world frame are given by

$$g^w = (0 \quad 0 \quad -g) \tag{6}$$
$$H^w = (a \quad 0 \quad b) \tag{7}$$

where g is the gravity and a and b are the components of the earth's magnetic field vector in the world frame.

If the initial state of the accelerometer is in the horizontal in the world frame, only the already-known component g_z^w of the gravity exists. After arbitrary rotation, the gravity at the current state can be obtained from the initial state using coordinate transformation with a DCM that contains the rotation angles (φ, θ, ψ). If the object is in static state, all the three gravity components can be measured using the accelerometer. By correlating the measured gravity of the current state to the initial state using coordinate transformation, the rotation angles can be solved.

From (3), the inverse transformation of the gravity is

$$g^b = R_w^b g^w \qquad R_w^b = (R_b^w)^T \tag{8}$$

where R_w^b is the DCM from the world frame to the body frame and equals to the transpose of matrix R_b^w. The superscript T represents the transpose of matrix. Substituting (5) and (6) into (8) and regarding the magnitude and the direction of the gravity as constant, one obtains

$$\begin{aligned} g^b &= \begin{pmatrix} g_x^b & g_y^b & g_y^b \end{pmatrix} \\ &= (-\sin\theta \quad \sin\varphi\cos\theta \quad \cos\varphi\cos\theta)(-g) \end{aligned} \tag{9}$$

where g_x^b, g_y^b, and g_z^b are the components of the gravity vector in the body frame.

Therefore, roll and pitch can be solved from the measured gravity vectors

$$\begin{aligned} \varphi &= \arctan\left(g_y^b / g_z^b\right) \\ \theta &= \arctan\left[-g_x^b / \left(g_y^b \sin\varphi + g_z^b \cos\varphi\right)\right] \end{aligned} \tag{10}$$

Equation (10) indicates that roll and pitch can be obtained from the gravity components at static state. This avoids the drift and the accumulated errors.

To determine yaw, the three components of the earth's magnetic field vector are needed. Using the roll and pitch that are already solved from (10), the main plane of the magnetometer can be transformed into the horizontal plane in the world frame through coordinate transformation. Then the earth's magnetic field vector in the horizontal plane can be transformed from the measured magnetic field vector

$$\begin{aligned} H^{hor} &= \begin{pmatrix} H_x^{hor} & H_y^{hor} & H_z^{hor} \end{pmatrix} = R(y,\theta)R(x,\varphi)H^w \\ R_w^b &= R(z,\psi)R(y,\theta)R(x,\varphi) \end{aligned} \tag{11}$$

where H^{hor} is the magnetic field vector when the magnetometer is in horizontal plane, and H_x^{hor}, H_y^{hor}, and H_z^{hor} are the three components. $R(x,\varphi)$, $R(y,\theta)$, and $R(z,\psi)$ are the rotation matrixes corresponding to x-, y-, and z-axis, respectively. Then yaw can be calculated using the following equation deduced from (11)

$$\psi = \arctan\left(H_y^{hor} / H_x^{hor}\right). \tag{12}$$

These equations allow the calculation of the components of the earth's magnetic field vector using roll, pitch, and the rotation matrix. In case of the existence of fast rotation or translational acceleration, the gravity components are indistinguishable from the unknown acceleration, and (10) is invalid for roll and pitch calculation. Hence, zero or small rotation and translational acceleration are the preliminary requirement for (10) and (12), i.e., in horizontal quasi or static state. For example, the rotation should be smaller than 5–10°/s to ensure the applicability of (10) and (12).

For dynamic state with remarkable rotation or translational acceleration, gyroscopes and accelerometers are employed to measure the dynamic rotation and to distinguish the translational acceleration. Although gyroscopes have drift for long-

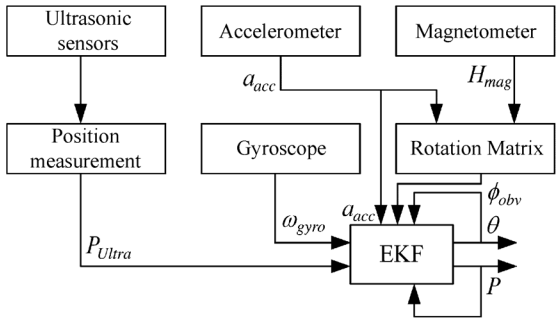

Fig. 4. EKF system.

term measurement, they are capable of measuring short-term rotation accurately. The results for zero roll and pitch are used as the observation of EKF to confine the gyroscope drift, which means that the orientation measured with gyroscopes is adopted to complement the digital compass in dynamic state in non-zero roll or pitch. This method relaxes the requirement of zero rotation or translational acceleration.

V. Extended Kalman Filter and Implementation

The proposed method uses a digital compass and a gyroscope for static state and dynamic state rotation determination, respectively, and uses ultrasonic sensors to calibrate the drift of accelerometers for position measurement. Fusing the data of the various types of sensors compensates the inefficacy of each sensor by other types of sensors [44]. For sensor data fusion, a classic approach to the state estimate problems for a nonlinear stochastic system is EKF [32], [35], which uses discrete models with first-order approximation for nonlinear systems. The EKF algorithm enables complementary compensation for each sensor's limitations, and the resulting performance of the sensor system is better than its any individual sensors. The state model and the observation model in EKF are established using kinematics.

A. System Structure

Fig. 4 shows the configuration of the EKF system. The position of the object P_{Ultra} is calculated using the ultrasonic sensor measured distances. The acceleration a_{acc} measured by the accelerometer and the earth's magnetic field H_{mag} measured by the magnetometer are used to determine the orientation ϕ_{obv}. The outputs of the accelerometer and the gyroscope, a_{acc} and ω_{gyro}, are used in the state equations to calculate the dynamic responses of the system.

The accelerometer and the gyroscope measure the object acceleration vector $(acc_x^b\ acc_y^b\ acc_z^b)$ and the angular rate $(\omega_x^b\ \omega_y^b\ \omega_z^b)$ with high sampling rates. These measurement data are transformed from the body frame to the world frame, followed by single or double integration to obtain linear acceleration $(a_x^b\ a_y^b\ a_z^b)$, velocity $(V_x^b\ V_y^b\ V_z^b)$, position $(S_x^b\ S_y^b\ S_z^b)$, and orientation $(\varphi^b\ \theta^b\ \psi^b)$.

B. State Model and Observation Model

As EKF uses discrete models, the kinematic equations are expressed in discrete form. The acceleration vector measured by the accelerometer is a sum of the gravity vector, the rotation acceleration, and the linear acceleration. Therefore, the acceleration is given by

$$\begin{bmatrix} a_x^b \\ a_y^b \\ a_y^b \end{bmatrix} = \begin{bmatrix} acc_x^b - \omega_y^b V_z^b + \omega_z^b V_y^b + g\sin\theta \\ acc_x^b + \omega_x^b V_z^b - \omega_z^b V_x^b - g\sin\varphi\cos\theta \\ acc_x^b - \omega_x^b V_y^b + \omega_y^b V_x^b - g\cos\varphi\cos\theta \end{bmatrix}. \quad (13)$$

The position and the velocity can be obtained from the acceleration using

$$V_{k+1}^b = V_k^b + a_k^b \Delta t \quad (14)$$

$$S_{k+1}^b = S_k^b + V_k^b \Delta t S^w = R_b^w S^b \quad (15)$$

where the subscripts k and $k+1$ indicate the values at time k and time $k+1$, respectively. a^b, V^b, S^b, and Δt are, respectively, the acceleration, velocity, position, and the sampling time.

The angular rates in the world frame can be calculated from the gyroscope using the following equations:

$$\begin{bmatrix} \omega_x^b \\ \omega_y^b \\ \omega_z^b \end{bmatrix} = \begin{bmatrix} \omega_x^w \\ 0 \\ 0 \end{bmatrix} + R^T(x,\varphi) \begin{bmatrix} 0 \\ \omega_x^w \\ 0 \end{bmatrix} + R^T(x,\varphi) R^T(y,\theta) \begin{bmatrix} 0 \\ 0 \\ \omega_x^w \end{bmatrix} \quad (16)$$

$$\begin{bmatrix} \omega_x^w \\ \omega_y^w \\ \omega_z^w \end{bmatrix} = R_b'^w(\theta)\omega^b = \begin{bmatrix} 1 & \sin\varphi\tan\theta & \cos\varphi\tan\theta \\ 0 & \cos\varphi & -\sin\varphi \\ 0 & \sin\varphi/\cos\theta & \cos\varphi/\cos\theta \end{bmatrix} \begin{bmatrix} \omega_x^b \\ \omega_y^b \\ \omega_z^b \end{bmatrix} \quad (17)$$

where $\omega_x^b, \omega_y^b, \omega_z^b$ and $\omega_x^w, \omega_y^w, \omega_z^w$ are the angular rates in the body frame and the world frame around x-, y-, and z-axis, respectively; $R^T(x,\varphi)$, $R^T(y,\theta)$, and $R_b'^w(\theta)$ are the transformation rotation matrixes from the body frame to the world frame for x-axis, y-axis, and angular rate, respectively.

Substituting (13) and (17) into (14) and noticing that $\theta_{k+1}^w = \theta_k^w + \omega^w \Delta t$, one obtains the state model from (14), (15) and (17)

$$\begin{bmatrix} S^w \\ V^b \\ \theta^w \end{bmatrix}_{k+1} = \begin{bmatrix} S_k^w + R_b^w(\theta)\left(V_k^b \Delta T\right) \\ V_k^b + \Delta T(a_k - \vec{g} - \vec{\omega} \times \vec{v})_k \\ \theta_k^w + R_b'^w(\theta)\omega_k^b \end{bmatrix} \quad (18)$$

where S^w, V^b, and θ^w are, respectively, the position in the world frame, the velocity in the body frame and the angles in the world frame; R_b^w and $R_b'^w$ are the frame transformation matrixes defined in (5) and (17).

The observation model involves the ultrasonic sensor, the accelerometer, and the magnetometer, and is given by

$$\begin{bmatrix} P_{Ultra} \\ \phi_{comp} \end{bmatrix} = \begin{bmatrix} 1 & 0 & 0 \\ 0 & 0 & 1 \end{bmatrix} \begin{bmatrix} S^w \\ V^b \\ \theta^w \end{bmatrix} \quad (19)$$

where P_{Ultra} is the position measured with the ultrasonic sensor and ϕ_{comp} is the rotation measured with the digital compass.

C. Implementation of EKF

EKF is a first-order approximation solution to nonlinear systems. For nonlinearity, a generic stochastic process is described by a discrete system

$$\begin{cases} x_{k+1} = f(x_k, u_k, v_k) \\ y_{k+1} = h(x_k, w_k) \end{cases} \tag{20}$$

where x_k and y_k are the state vector and the observation vector, respectively; f and h are the state function and the observation function, respectively; u_k is the system input, v_k and w_k are the white Gaussian noise and the measurement noise with different covariance matrix Q_k and R_k, respectively. The state and the observation functions are linearized using the following equations

$$A_{[i,j]} = \frac{\partial f_{[i]}}{\partial x_{[j]}} \qquad H_{[i,j]} = \frac{\partial h_{[i]}}{\partial x_{[j]}} \tag{21}$$

where A and H are the Jacobian matrixes of the state and the observation functions, respectively. Neglecting the high-order terms of Taylor series, the *priori* state estimate and the covariance matrix are given as

$$\begin{aligned} x_{k+1}^{-} &= f\left(x_k^{+}, u_k, 0\right) \\ P_{k+1}^{-} &= A_k P_k A_k^T + Q_k \end{aligned} \tag{22}$$

where x_{k+1}^{-}, P_{k+1}^{-}, and x_k^{+} are the *priori* state at time k, the *priori* covariance at time $k+1$, and the *posteriori* state at time k, respectively. From the prediction (22), the *posteriori* estimate is given by

$$\begin{aligned} K_{k+1} &= P_{k+1}^{-} H_k^T \left(H_k P_{k+1}^{-} H_k^T + R_k\right)^{-1} \\ x_{k+1}^{+} &= x_{k+1}^{-} + K_{k+1}\left(z_{k+1} - H_k x_{k+1}^{-}\right) \\ P_{k+1}^{+} &= (I - K_{k+1} H_k) P_{k+1}^{-} \end{aligned} \tag{23}$$

where K_{k+1}, x_{k+1}^{+}, and P_{k+1}^{+} are, respectively, the Kalman gain, the *posteriori* estimate, and the *posteriori* covariance. EKF is implemented using (20)–(23) to estimate the state and to complement different sensors.

VI. Experimental Results

A. Experiments

A test vehicle is constructed and EKF is implemented to verify the function of motion measurement and the capability of reducing the accumulated errors of inertial sensors. The test vehicle is a small box with a printed circuit board (PCB) for signal processing packaged, on which a three-axis accelerometer (ST), a three-axis gyroscope (InvenSense), a triad of magnetometers (Yamaha), and an ultrasonic sensor are fixed. An ARM processor and a C-program are used for data processing and EKF algorithm.

Fig. 5 shows the principle of the test vehicle. The signals of the acceleration and the angular rate are converted by AD and input to the processor. The magnetometer communicates with the processor using IIC bus, and the processor is connected to the computer though RS232. The processor controls the ultrasonic emitter through pulse width modulation. When the ultrasonic receiver receives ultrasonic wave, an interrupt is generated to record the distance between the emitter and the receiver. EKF is implemented by the processor to calculate the position and the orientation. The sampling rate is 25 Hz.

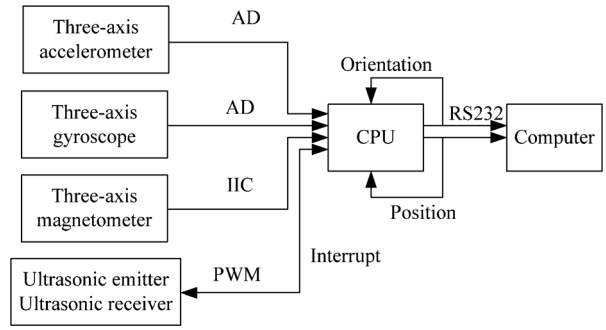

Fig. 5. Principle and the configuration of the test vehicle.

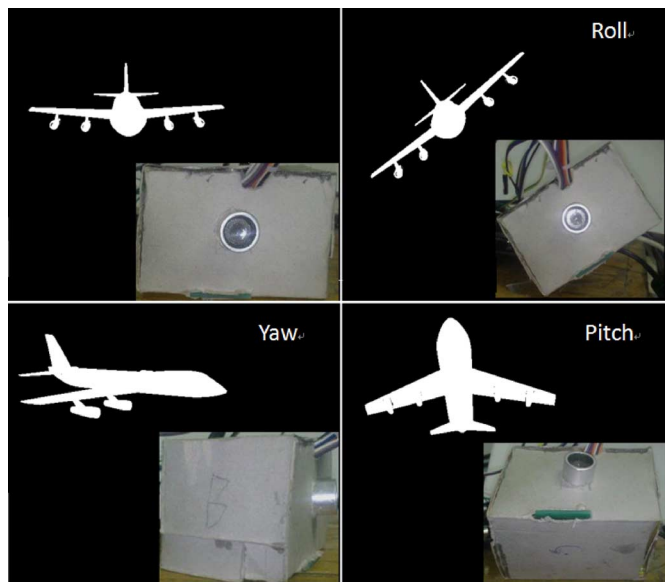

Fig. 6. Snapshot of the real-time orientation demo system.

The first step is to operate the sensors at static state to calculate the attitude initials, and after convergence the results are used for the following dynamic test by setting the velocity to zero. Four dynamic experiments are performed to validate the proposed approach and the test vehicle. First, a simple demo system is constructed to verify the function and the feasibility of the method. Second, the digital compass and the gyroscope are evaluated for orientation determination in both static state and dynamic state. Third, the accelerometer and the ultrasonic sensor are tested for position measurement. Last, the test vehicle is compare with a commercial product.

B. System Verification

A real-time demo system including the test vehicle and software is constructed to verify the function of the test vehicle in orientation determination. Fig. 6 uses the attitudes of an airplane

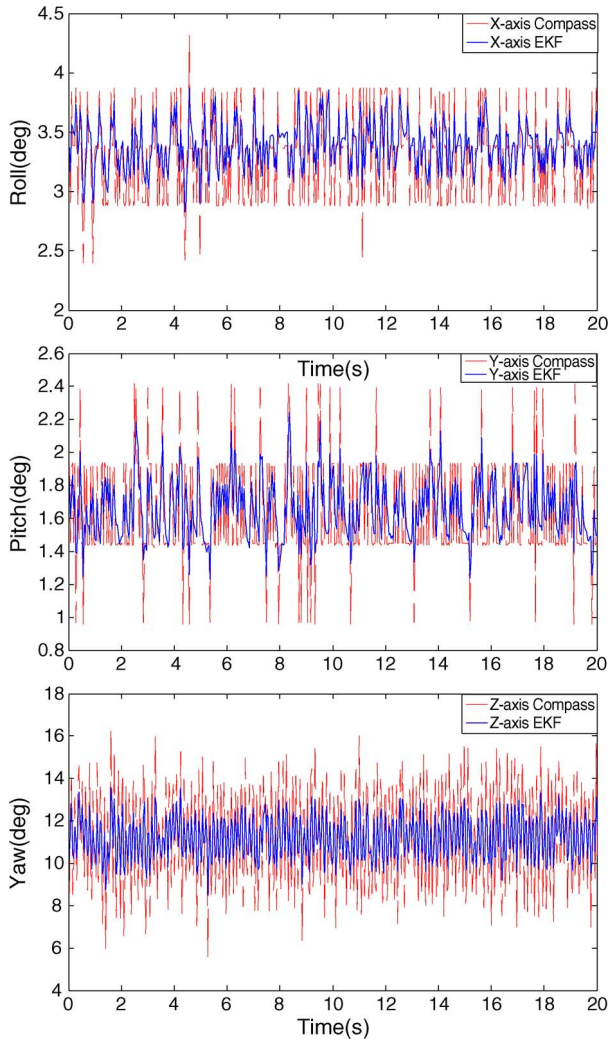

Fig. 7. Static orientation measurement with compass and EKF.

to synchronously indicate the attitudes of the demo system. The orientations of the demo system in dynamic state are calculated from the measured results using EKF data fusion, and are represented by the airplane attitudes. For clarity, roll, pitch, and yaw are introduced to the orientation observation separately and shown by the airplane independently. The orientation changes of the airplane are consistent and synchronous with the demo system, verifying the effectiveness of the demo system and the EKF algorithm.

C. Orientation Measurement Results

Fig. 7 shows the three axes orientations in static state measured by the digital compass and by the EKF fused digital compass and gyroscope (DCG). In static state the orientations measured using the digital compass and EKF fused DCG are stable and the orientation deviations are rather small. Compared with IMUs [33], the digital compass and EKF fused DCG achieve high accuracy for orientation measurement. The digital compass measures the gravity and the earth's magnetic field vector, and the orientation is calculated using rotation matrix from the world frame to the body frame. In this procedure, anti-trigonometric function is employed to calculate the orientations to avoid integration induced accumulated errors. The integration-free and the time-independent properties allow small deviations for long-term measurement.

TABLE I
STATIC ORIENTATION VARIANCE OF DIGITAL COMPASS AND EKF

Static	x-axis (°)	y-axis (°)	z-axis (°)
Digital compass	0.3425	0.3111	2.3172
DCG EKF	0.1915	0.1769	1.0314
Improvement	44.1%	43.1%	55.5%

It can be seen from Fig. 7 that the overall deviations in the orientation of each axis obtained using the DCG EKF are much smaller than those measured using the digital compass, in particular for the large deviations of the digital compass. The average variance measured using the two methods are listed in Table I for comparison. The DCG EKF reduces the orientation variances of the x-, y-, and z-axis to around 55%, 57%, and 44% of the corresponding variances measured using the digital compass. The results show that the proposed DCG EKF is effective in noise reduction and enables significant accuracy improvement in orientation measurement.

Fig. 8 shows the orientations of the three axes in dynamic state measured using the digital compass and the DCG EKF. In dynamic test, the object is subjected to rotation with angles of 45°, 45°, and 90° around x-, y-, and z-axis, respectively. It can be seen that significant peaks, i.e., measurement errors, appear in the digital compass at the beginning and end of each rotation around x- and y-axis. Although the data converge after 100–200 ms and reach stable state, the peaks represent rotation errors as much as 10°–30° for x- and y-axis. This indicates that large roll and pitch measurement errors occur in dynamic state when the object rotates rapidly because the accelerometer is unable to distinguish the gravity from the extra acceleration. By using DCG EKF, large roll and pitch measurement errors, i.e., the peaks, are substantially reduced because the gyroscope instead of the digital compass measures the short-term orientation when rotation or acceleration is detected. The EKF not only significantly reduces the large errors at the moment of rotation, but also smoothes the platforms between two rotations by reducing the deviations. It can be concluded that for orientation measurement in dynamic state the proposed approach using multi-sensors and EKF algorithm constrains the accumulated errors that are inevitable in IMUs.

Table I shows that DCG EKF is more effective in reducing the measurement variance of z-axis rotation than the other two axes. This indicates that introducing gyroscopes and EKF is of great help to improve the yaw measurement accuracy. This can be attributed to the measurement of rotation using gyroscopes or the transient translational acceleration using accelerometer. However, the absolute errors and the ripples of z-axis are larger than the other two axes. This can be expected because the z-axis calculation is based on the rotation measurement results of x- and y-axis, and therefore the errors of z-axis are larger than those of x- and y-axis.

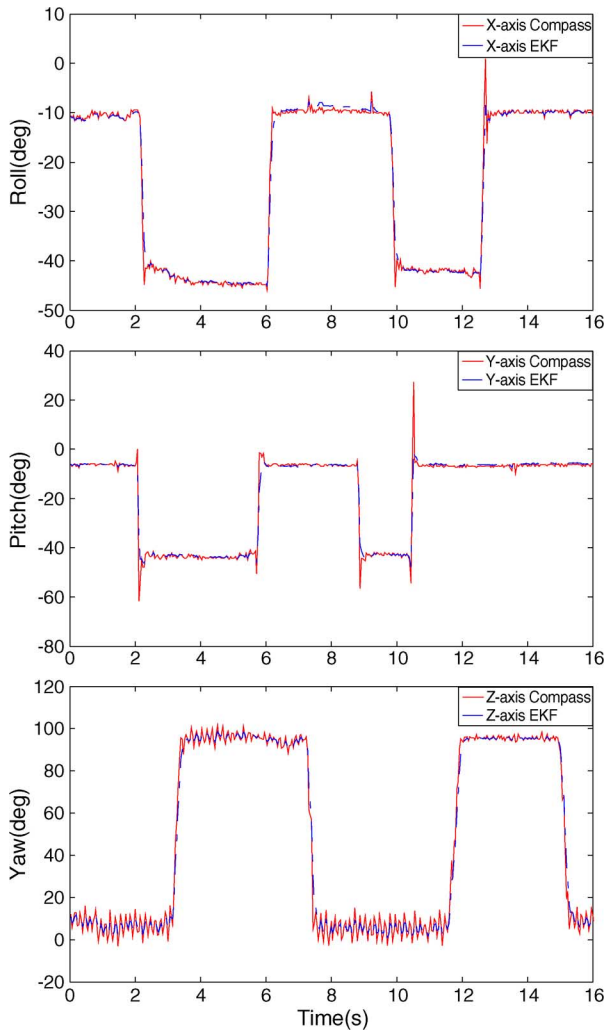

Fig. 8. Dynamic orientation measurement with compass and EKF.

TABLE II
STATIC POSITION VARIANCE USING ULTRASONIC SENSORS

Static	x-axis (m)	y-axis (m)	z-axis (m)
Position	1.9909e-4	2.0296e-4	2.8979e-4

D. Position Measurement Results

For position measurement through double integration of acceleration, the drift of the accelerometers and the double integration result in significant position measurement errors [33]. Fig. 9 shows the divergence in position measurement induced by drift. Without the ultrasonic sensor (disabled), the position obtained using double integration for static state diverges rapidly and randomly from zero with a speed of 0.25–0.5 m/s. High grade accelerometers are beneficial to reducing the drift induced errors. When the ultrasonic sensor is enabled, the measured position immediately returns to the ultrasonic sensor measured values, and the drift induced accumulated errors are eliminated. These results show that the position measurement using accelerometers can be compensated by ultrasonic sensors using EKF data fusion.

Fig. 10 shows the position measurement results in static state using ultrasonic sensor calibration through EFK data fusion.

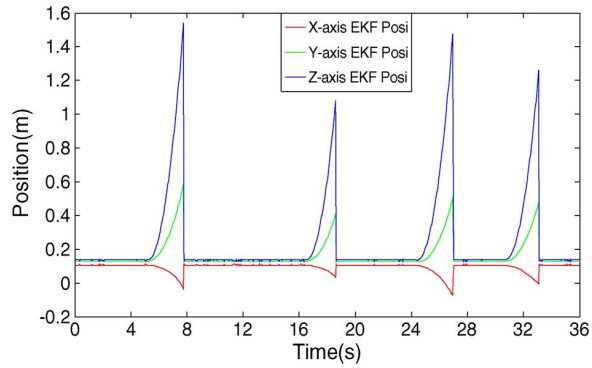

Fig. 9. Calibration effects of the ultrasonic sensor on position measurement through double integration of acceleration.

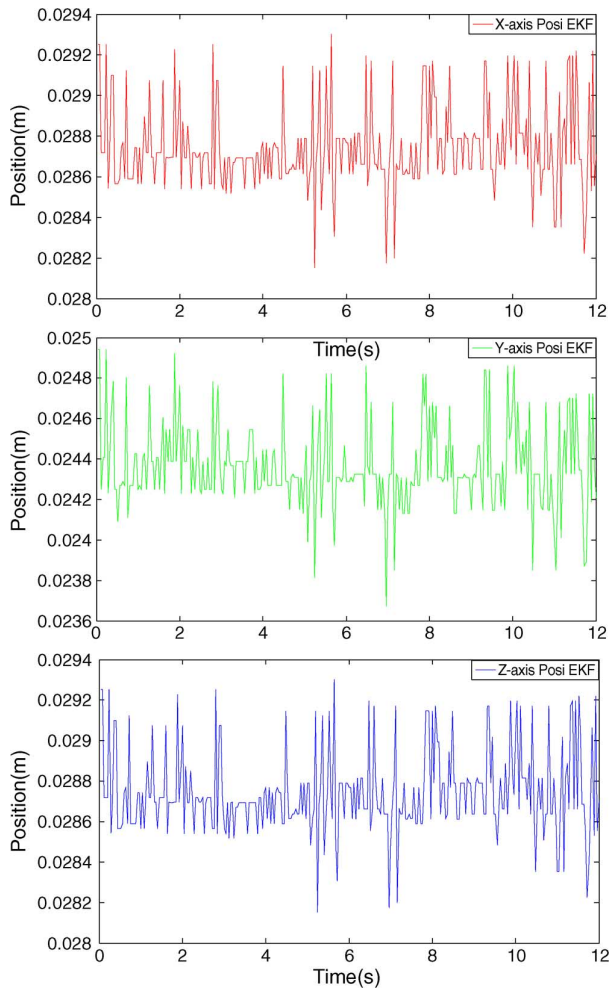

Fig. 10. Static position measurement using ultrasonic sensors and EKF data fusion.

The absolute and the relative drifts are, respectively, within 0.03 m and 0.001 m for x- and y-axis, and 0.12 m and 0.0016 m for z-axis. Table II shows the average position deviations of the three axes using EKF data fusion. It can be concluded that the ultrasonic sensors, which directly measure the absolute positions in a time-independent manner, are free of drift and accumulated errors. It should be noted that because the object is still moving during the propagation of ultrasonic waves, the position calculated using the ultrasonic sensor corresponds to the moment of

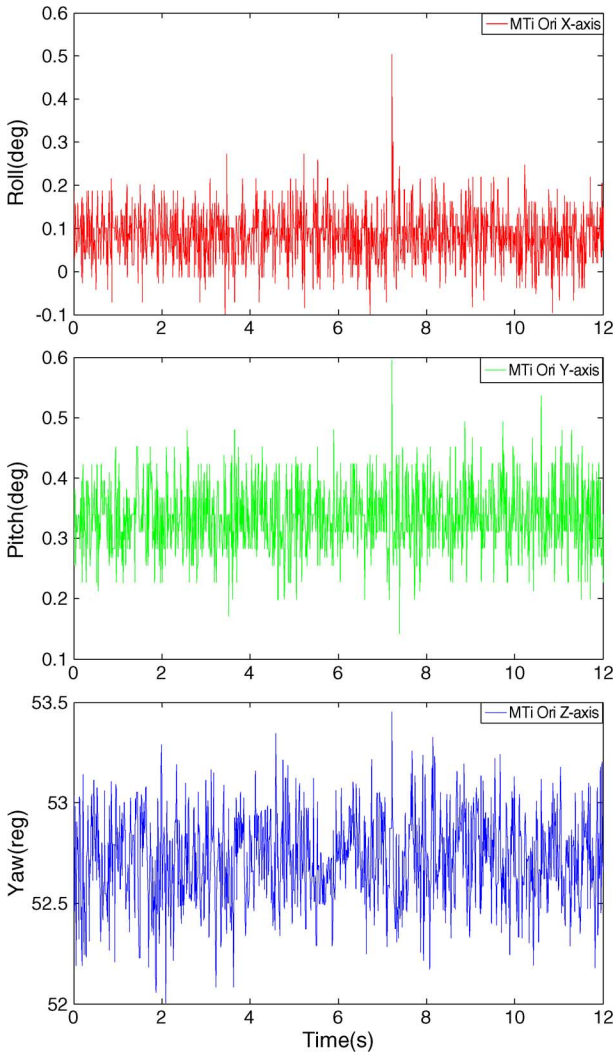

Fig. 11. Orientation measurement using MTi IMU.

ultrasonic signal emitting rather than receiving. For a speed of 1 m/s, the position changes during signal traveling are about 1 cm, which is acceptable for indoor robot applications.

E. Comparison With a Commercial Product

The test vehicle is compared with a commercial product, MTi IMU module from Xsens Company. The MTi consists of a tri-axis accelerometer, a tri-axis gyroscope, a tri-axis magnetometer, a temperature sensor, and a GPS module. The sensor output is processes by a 16-bit ADC, and the data are fused using Xsens Kalman filter (XKF).

Fig. 11 shows the orientation around the three axes in static state measured with XKF. The maximum swing amplitudes are within 0.3° for x- and y-axis, and 1.2° for z-axis. These results are about 3–4 times better than the test vehicle. Table III compares the variances of the test vehicle with MTi. It can be seen that the variance of MTi is about 3–5 times smaller than our test vehicle. This could be attributed to the superior grade of the sensors used in the MTi module. However, the price of the MTi module is about 20 times higher than the cost of our test vehicle.

TABLE III
COMPARISON WITH MTI IMU MODULE

	x-axis (°)	y-axis (°)	z-axis (°)
DCG EKF	0.1915	0.1769	1.0314
MTi XKF	0.0476	0.0481	0.3062
MTi EKF	0.0226	0.0189	0.0507

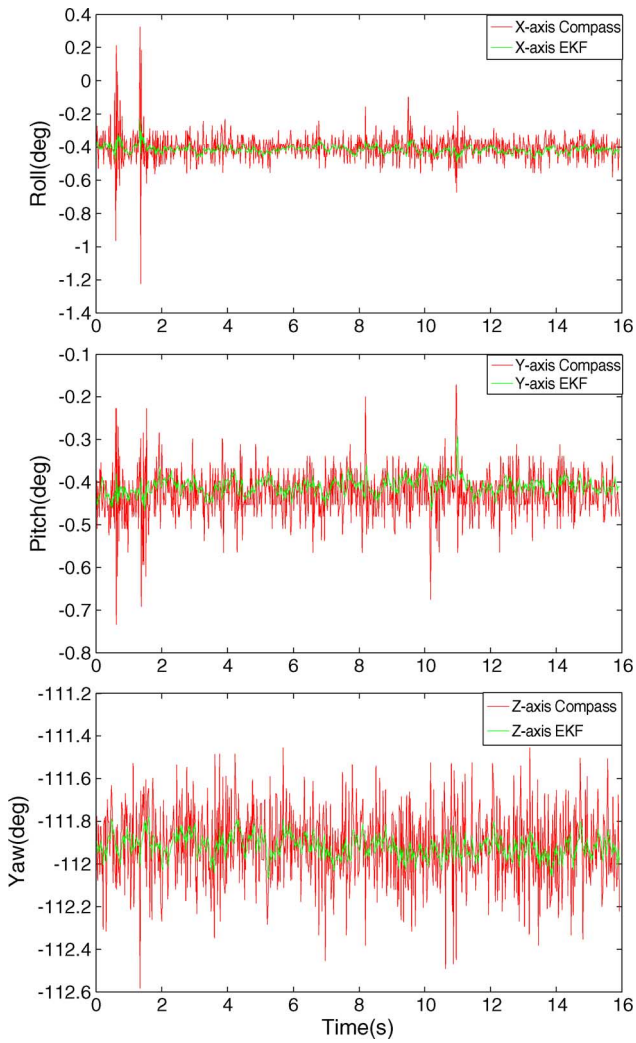

Fig. 12. Orientation measurement using MTi XKF and MTi EKF.

To validate our EKF algorithm and compare the sensor grade of the MTi module with those of the test vehicle, the output signals of the MTi sensors are intercepted and processed using our EKF, such that the EKF uses two different sets of multi-sensors to compare the sensor grade. Fig. 12 shows the swing amplitudes of the orientations measured using MTi XKF and MTi EKF. It can be seen that the swing amplitudes of MTi EKF are smaller than those of MTi XKF. Table III lists the variances of the DCG EKF, MTi XKF, and MTi EKF. Using the MTi sensors and the EKF algorithm, the variances of x-, y-, and z-axis orientations are 47%, 39%, and 17% of those of MTi XKF, respectively, and are 12%, 11%, and 5% of those of DCG EKF, respectively. These results validate the proposed method in motion determination.

VII. Conclusion

A sensor system for position and orientation determination has been developed using complementary accelerometers, gyroscopes, magnetometers, and ultrasonic sensors. A gyroscope that is able to measure transient rotation is used to compensate the digital compass in case of rotation or translational acceleration. This combination takes the advantages of the digital compass in accumulated error-free measurement in static state and the short-term accuracy of the gyroscope in dynamic state. Ultrasonic sensors are used to calibrate the drift of accelerometers in position measurement, and the accelerometer complements the low sampling rate of ultrasonic sensor and works independently when the ultrasonic signals are temporarily not available. Experimental results demonstrate that the multi-sensors can measure position and orientation with lower uncertainties after EKF data fusion.

Acknowledgment

The authors would like to thank Yamaha (Shanghai) for donating the magnetic sensors and the signal processing circuit board. The authors thank Dr. J. Hofschulte and Dr. J. Li from ABB Research for their helpful discussions.

References

[1] T. Liu, Y. Inoue, K. Shibata, and X. Tang, "A wearable inertial sensor system for human motion analysis," in *Proc. 2005 IEEE Comput. Intell. Symp. Robot. Autom.*, 2005, pp. 409–413.

[2] T. Lee, J. Shin, and D. Cho, "Position estimation for mobile robot using in-plane 3-axis IMU and active beacon," in *Proc. IEEE Ind. Electron.*, 2009, pp. 1956–1961.

[3] J. S. Wang, Y. L. Hsu, and J. N. Liu, "An inertial-measurement-unit-based pen with a trajectory reconstruction algorithm and its applications," *IEEE Trans. Ind. Electron.*, vol. 57, pp. 3508–3521, 2010.

[4] S. Zhou, Z. Dong, W. J. Li, and C. P. Kwong, "Hand-written character recognition using MEMS motion sensing technology," in *Proc. IEEE/ASME Int. Conf. Adv. Intell. Mechatronics*, 2008, pp. 1418–1423.

[5] S. H. P. Won, F. Golnaraghi, and W. W. Melek, "A fastening tool tracking system using an IMU and a position sensor with Kalman filters and a fuzzy expert system," *IEEE Trans. Ind. Electron.*, vol. 56, no. 5, pp. 1782–1792, May 2009.

[6] A. K. Brown, "GPS/INS uses low-cost MEMS IMU," *IEEE Aero. Electron. Syst. Mag.*, vol. 20, no. 9, pp. 3–10, Sep. 2005.

[7] G. C. Karras and K. J. Kyriakopoulos, "Localization of an underwater vehicle using an IMU and a laser-based vision system," in *Proc. Mediterranean Conf. Cont. Autom.*, 2007, pp. 1–6.

[8] D. I. B. Randeniya, S. Arkar, and M. Gunaratne, "Vision-IMU integration using a slow-frame-rate monocular vision system in an actual roadway setting," *IEEE Trans. Intell. Transp. Syst.*, vol. 11, no. 2, pp. 256–266, Jun. 2010.

[9] J. Kelly and G. S. Sukhatme, "Visual-inertial simultaneous localization, mapping and sensor-to-sensor self-calibration," in *Proc. IEEE Int. Symp. Comput. Intell. Robot. Autom.*, 2009, pp. 360–368.

[10] S. H. Won, W. Melek, and F. Golnaraghi, "Position and orientation estimation using Kalman filtering and particle filtering with one IMU and one position sensor," in *IEEE Conf. Ind. Electron.*, 2008, pp. 3006–3010.

[11] S. H. P. Won, W. W. Melek, and F. Golnaraghi, "A Kalman/particle filter-based position and orientation estimation method using a position sensor/inertial measurement unit hybrid system," *IEEE Trans. Ind. Electron.*, vol. 57, pp. 1787–1798, 2010.

[12] S. Beiter, R. Poquette, B. S. Filipo, and W. Goetz, "Precision hybrid navigation system for varied marine applications," in *Proc. IEEE Position Location Navigation Symp.*, 1998, pp. 316–323.

[13] P. M. Lee, B. H. Jun, K. Kim, J. Lee, T. Aoki, and T. Hyakudome, "Simulation of an inertial acoustic navigation system with range aiding for an autonomous underwater vehicle," *IEEE J. Oceanic Eng.*, vol. 32, no. 2, pp. 327–345, Apr. 2007.

[14] E. Foxlin and L. Naimark, "VIS-tracker: A wearable vision-inertial self-tracker," in *Proc. IEEE Virtual Reality*, 2003, pp. 199–206.

[15] F. Aghili, M. Kuryllo, G. Okouneva, and C. English, "Fault-tolerant position/attitude estimation of free-floating space objects using a laser range sensor," *IEEE Sens. J.*, vol. 11, no. 1, pp. 176–185, Jan. 2011.

[16] J. Lobo and J. Dias, "Relative pose calibration between visual and inertial sensors," *Int. J. Robot. Res.*, vol. 26, pp. 561–575, 2007.

[17] D. Lin, K. V. Ling, G. R. Hu, and N. Nagarajan, "GPS-based attitude determination for microsatellite using three-antenna technology," in *Proc. IEEE Aerospace Conf.*, 2004, vol. 2, pp. 1024–1029.

[18] L. Whitcomb, D. Yoerger, and H. Singh, "Advances in Doppler-based navigation of underwater robotic vehicles," in *IEEE Int. Conf. Robot. Automat.*, 1999, pp. 399–406.

[19] E. Ivanjkl, M. Vasak, and I. Petrovic, "Kalman filter theory based mobile robot pose tracking using occupancy grid maps," in *Proc. Int. Conf. Control Automat.*, 2005, pp. 869–874.

[20] L. Tamás, G. Lazea, R. Robotin, C. Marcu, S. Herle, and Z. Szekely, "State estimation based on Kalman filtering techniques in navigation," in *IEEE Conf. Automat. Quality Testing Robot.*, 2008, pp. 147–152.

[21] H. P. Henderson and D. M. Bevly, "Relative position of UGVs in constrained environments using low cost IMU and GPS augmented with ultrasonic sensors," in *Proc. IEEE/ION Position Location Navigation Symp.*, 2008, pp. 1269–1277.

[22] H. Kim and J. Chio, "Advanced indoor localization using ultrasonic sensor and digital compass," in *Proc. Int. Conf. Contr. Autom. Syst.*, 2008, pp. 223–226.

[23] Z. Dong, G. Zhang, C. C. Tsang, G. Shi, W. J. Li, P. H. W. Leong, and M. Y. Wong, "μIMU-based handwriting recognition calibration by optical tracking," in *Proc. 2007 IEEE Int. Robot. Biomimetics Conf.*, pp. 382–387.

[24] F. M. Mirzaei and S. I. Roumeliotis, "A Kalman filter-based algorithm for IMU-camera calibration: Observability analysis and performance evaluation," *IEEE Trans. Robot.*, vol. 24, pp. 1143–1156, 2008.

[25] V. Sazdovski and P. M. G. Silson, "Inertial navigation aided by vision-based simultaneous localization and mapping," *IEEE Sensors J.*, accepted for publication.

[26] R. Zhu and Z. Zhou, "A real-time articulated human motion tracking using tri-axis inertial/magnetic sensors package," *IEEE Trans. Neural Syst. Rehabilitation Eng.*, vol. 12, pp. 295–302, 2004.

[27] M. Di, E. M. Joo, and L. H. Beng, "A comprehensive study of Kalman filter and extended Kalman filter for target tracking in wireless sensor networks," in *Proc. IEEE Conf. Syst. Man Cybernetics*, 2008, pp. 2792–2797.

[28] J. L. Marins, X. Yun, E. R. Bachmann, R. B. McGhee, and M. J. Zyda, "An extended Kalman filter for quaternion-based orientation estimation using MARG sensors," in *IEEE Int. Conf. Intell. Robots Syst.*, 2001, vol. 4, pp. 2003–2011.

[29] R. Toledo-Moreo, M. A. Zamora-Izquierdo, and A. F. Gómez-Skarmetra, "IMM-EKF based road vehicle navigation with low cost GPS/INS," in *IEEE Int. Conf. Multisensor Fusion Integration Intell. Syst.*, 2006, pp. 433–438.

[30] A. Kim and M. F. Golnaraghi, "A quaternion-based orientation estimation algorithm using an inertial measurement unit," in *Proc. Position Location Navigation Symp.*, 2004, pp. 268–272.

[31] E. R. Bachmann, X. Yun, D. McKinney, R. B. McGhee, and M. J. Zyda, "Design and implementation of MARG sensors for 3-DOF orientation measurement of rigid bodies," in *Proc. IEEE Int. Conf. Robot. Autom.*, 2003, vol. 1, pp. 1171–1178.

[32] X. Yun and E. R. Bachmann, "Design, implementation, and experimental results of a quaternion-based Kalman filter for human body motion tracking," *IEEE Trans. Robot.*, vol. 22, pp. 1216–1227, 2006.

[33] D. Li, R. Landry, and P. Lavoie, "Low-cost MEMS sensor-based attitude determination system by integration of magnetometers and GPS: A real-data test and performance evaluation," in *Proc. IEEE/ION Position, Location Navigation Symp.*, 2008, pp. 1190–1198.

[34] D. Vissière, A. Martin, and N. Petit, "Using distributed magnetometers to increase IMU-based velocity estimation into perturbed area," in *Proc. 46th IEEE Conf. Decision Control*, 2007, pp. 4924–4931.

[35] A. M. Sabatini, "Quaternion-based extended Kalman filter for determining orientation by inertial and magnetic sensing," *IEEE Trans. Biomed. Eng.*, vol. 53, pp. 1346–1356, 2006.

[36] B. Huyghe, J. Doutreloigne, and J. Vanfleteren, "3D orientation tracking based on unscented Kalman filtering of accelerometer and magnetometer data," in *Proc. IEEE Sensors Appl. Symp.*, 2009, pp. 148–152.

[37] T. Harada, H. Uchino, T. Mori, and T. Sato, "Portable orientation estimation device based on accelerometer, magnetometers and gyroscope sensors for sensors network," in *Proc. IEEE Int. Conf. Multisensor Fusion Integration Intelligent Systems*, 2003, pp. 191–196.

[38] Y. Luo, C. C. Tsang, and G. Zhang *et al.*, "An attitude compensation technique for a MEMS motion sensor based digital writing instrument," in *Proc. IEEE Conf. Nano/Micro Eng. Molecular Syst.*, 2006, pp. 909–914.
[39] D. Roetenberg, P. J. Slycke, and P. H. Veltink, "Ambulatory position and orientation tracking fusing magnetic and inertial sensing," *IEEE Trans. Biomed. Eng.*, vol. 54, pp. 883–890, 2007.
[40] M. Wang, Y. Yang, R. R. Hatch, and Y. Zhuang, "Adaptive filter for a miniature MEMS based attitude and heading reference system," in *Proc. IEEE Position Location Navigation Symp.*, 2004, pp. 193–200.
[41] X. Yun, M. Lizarraga, E. R. Bachmann, and R. B. McGhee, "An improved quaternion-based Kalman filter for real-time tracking of rigid body orientation," in *Proc. IEEE Conf. Intell. Robots Syst.*, 2003, vol. 2, pp. 1074–1079.
[42] B. Mao and J. Wu, "An adaptive particle filter for MEMS based SINS non-linear initial alignment," in *Proc. IEEE Int. Conf. Infor. Automat.*, 2010, pp. 1504–1509.
[43] Y. S. Suh, "Orientation estimation using a quaternion-based indirect Kalman filter with adaptive estimation of external acceleration," *IEEE Trans. Instrum. Meas.*, vol. 59, no. 12, pp. 3296–3305, Dec. 2010.
[44] S. B. Lazarus, I. Ashokaraj, A. Tsourdos, R. Zbikowski, P. M. G. Silson, N. Aouf, and B. A. White, "Vehicle localization using sensors data fusion via integration of covariance intersection and interval analysis," *IEEE Sens. J.*, vol. 7, no. 9, pp. 1302–1314, Sep. 2007.
[45] A. Nemra and N. Aouf, "Robust INS/GPS sensors fusion for UAV localization using SDRE nonlinear filtering," *IEEE Sens. J.*, vol. 10, no. 4, pp. 789–798, Apr. 2010.

He Zhao was born in China in 1985. He received the B.S. degree in automatic control from North China University of Technology, Beijing, China, in 2007, and M.S. degree in Integrated Circuit Engineering from Institute of Microelectronics, Tsinghua University, Beijing, China, in 2011.

He is now with Beijing Aerospace Times Optical-Electronic Technology Co., Ltd.. His research interests are MEMS sensors and multi-sensor data fusion.

Zheyao Wang (M'07) was born in China in 1972. He received the B.S. degree in mechanical engineering in 1995, and the Ph.D. degree in mechatronics in 2000, both from Tsinghua University, Beijing, China.

From 2000 to 2002, he was a Postdoctoral Research Fellow at the Institute of Microelectronics, Tsinghua University, where he worked on silicon micromachining for microsensor applications. In 2002, he joined DIMES, Delft University of Technology, Delft, the Netherlands, as a Postdoctoral Researcher, and worked on silicon micromachining for 3-D packaging. He currently is a Full Professor at Tsinghua University. His research interests include microsensors, silicon micromachining, and MEMS. He has published more than 60 peer-reviewed journal and conference papers, and severs as a technical program committee member for IEEE Sensors Conference since 2008.